International Journal of Systems Science, 2001, volume 32, number 4, pages 523–532

Adaptive friction compensation of servo mechanisms

S. S. Ge†, T. H. Lee‡ and S. X. Ren‡

In this paper, adaptive friction compensation is investigated using both model-based and neural network (non-model-based) parametrization techniques. After a comprehensive list of commonly used models for friction is presented, model-based and non-model-based adaptive friction controllers are developed with guaranteed closed-loop stability. Intensive computer simulations are carried out to show the effectiveness of the proposed control techniques, and to illustrate the effects of certain system parameters on the performance of the closed-loop system. It is observed that as the friction models become complex and capture the dominate dynamic behaviours, higher feedback gains for model-based control can be used and the speed of adaptation can also be increased for better control performance. It is also found that neural networks are suitable candidate for friction modelling and adaptive controller design for friction compensation.

1. Introduction

Friction exists in all machines having relative motion and plays an important role in many servo mechanisms and simple pneumatic or hydraulic systems. It is a natural phenomenon that is quite hard to model, if not impossible. As friction does not readily yield to rigorous mathematical treatment, it is often simply ignored for the lack of control tools available or regarded as a phenomenon unworthy of discussion. In reality, friction can lead to tracking errors, limit cycles and undesired stick–slip motion. Engineers have to deal with the undesirable effects of friction although there is a lack of effective tools to make it easier to handle.

All surfaces are irregular at the microscopic level, and in contact at a few asperity junctions as shown in figure 1. These asperities behave like springs and can deform either elastically or plastically when subjected to a shear force. Thus, friction will act in the direction opposite to motion and will prevent true sliding from taking place as long as the tangential force is below a certain stiction limit at which the springs become deformed plastically. At the macroscopic level, many factors affect friction such as lubrication, the velocity, the temperature, the force orthogonal to the relative motion and even the history of motion. In an effort to deal with the undesired effects of friction effectively, many friction models have been presented in the literature relevant to friction modelling and control.

Friction is highly nonlinear and very hard to model completely if not impossible. This is especially true at the micrometre level. The notorious components in frictional are stiction and Coulomb frictional forces, which are highly nonlinear functions of velocity although bounded and cannot be handled by linear control theory. Traditionally, friction is treated as a bounded disturbance, and the standard proportional–integral–derivative (PID) algorithm is used in motion control. However, the integral control action may cause limit cycles around a target position and cause large tracking errors. If only proportional–derivative (PD) control is employed, then friction will cause a finite steady-state error. Although high-gain PID can reduce the steady-state position error due to friction, it often causes system instability when the drive train is compliant (Dupont 1994). Thus, in order to achieve high-precision motion control, friction must be appropriately compensated for. Friction compensation can be achieved on the basis of a reasonably accurate model for friction. However, it is difficult to model friction because it depends on the velocity, the position, the temperature, lubrication and even the history of motion. Direct compensation of fric-

Received 16 March 1999. Revised 21 February 2000. Accepted 10 March 2000.

† Department of Electrical Engineering, National University of Singapore, Singapore 117576. Tel: (+65) 874 6821, Fax: (+65) 779 1103, e-mail: elegesz@nus.edu.sg.

‡ Department of Electrical Engineering, National University of Singapore, Singapore 117576.

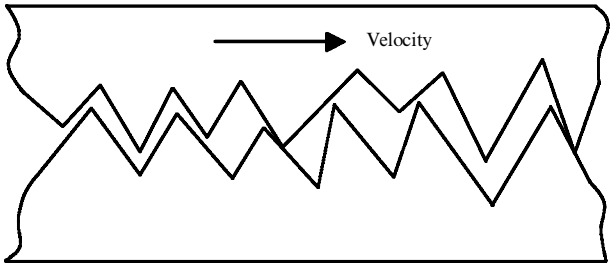

Figure 1. A microscopic view of the friction phenomenon.

tion is desirable and effective in motion control. However, it is difficult to realize in practice because of the difficulty in obtaining a truly representative parametric model. For controller design, the parametric model should be simple enough for analysis, and complex enough to capture the main dynamics of the system. If the model used is too simple, such as the simple Coulomb friction and viscous friction model, then there is the possibility of over compensation resulting from estimation inaccuracies (Canudas de Wit *et al.* 1991). Adaptive friction compensation schemes have been proposed to compensate for nonlinear friction in a variety of mechanisms (Canudas de Wit *et al.* 1991, Annaswamy *et al.* 1998), but these are usually based on the linearized model or a model which is linear in the parameters (LIP) for the problems under study. Each model only captures the dominate friction phenomena of the actual nonlinear function and may exhibit discrepancies when used for other systems where other friction phenomena dominate.

Thus neural networks can approximate any continuous nonlinear function to any desired accuracy over a compact set. As an alternative, neural networks can be used to parametrize the nonlinear friction and subsequently, adaptive control can be incorporated for on-line tuning. The resulting schemes is non-model based and does not require the exact friction model which is difficult to obtain in practice. Canudas de Wit and Ge (1997) have used neural networks to approximate the nonlinear function in the Z model. Kim and Lewis (1998) applied adaptive multilayer neural networks to the control of servo mechanisms.

In this paper, after reviewing all the commonly used friction models for controller design and simulation, we shall present a simple LIP friction model that captures most of the observed friction phenomena and is easy to use for controller design. As the space of primitive function increases, the model becomes more complete and representative and thus reduces the possibility of friction over-compensation resulting from estimation inaccuracies caused by simplified friction model structures such as the Coulomb friction and viscous friction model. To reduce further the work load in obtaining a complete dynamic model, neural networks are also used to model the dynamic friction. For ease of comparison and uniformity, only LIP neural networks are investigated while multilayer neural networks can also be similar applied without much difficulty (Lewis and Liu 1996, Zhang *et al.* 1999). Finally, extensive simulation studies are presented to show the effectiveness of the proposed control methods and the effects in augmenting primitive function space.

2. System and dynamic modelling

2.1. *Dynamic system*

A large class of servo mechanisms can be represented by a simple mass system as shown in figure 2. The dynamic equation of the system is given by

$$m\ddot{x} + f(x, \dot{x}) + d(t) = u, \tag{1}$$

where m is the mass, x is the displacement, u is the control force, $f(x, \dot{x})$ is the frictional force to be described in detail and $d(t)$ is the external disturbance which is assumed to be bounded by $b_d > 0$ as

$$|d(t)| \leqslant b_d. \tag{2}$$

2.2. *Friction models*

It is well known that friction depends on both the velocity and the position, but its structure is not well defined especially at low velocities. For ease of analysis and simulation, it is important to have a mathematical model of friction. A friction model should be able to predict accurately the observed friction characteristics, and simple enough for friction compensation.

Friction is a multifacetted phenomenon and exhibits the well-known classical Coulomb and viscous friction, nonlinearity at low velocities, and elasticity of the contact surfaces. In any given circumstance, some features may dominate over others and some features may not be detectable with the available sensing technology, but all these phenomena are present all the time. The use of a more complete friction model will extend the applicability of analytical results and will resolve discrepancies

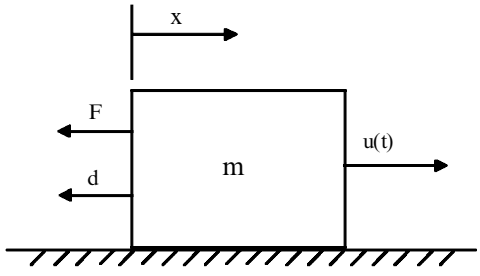

Figure 2. A dynamic system.

that arise in different investigations. While the classical friction models give only the static relationships between the velocity and the frictional force, the most recent friction model, the so-called Z model, is dynamic with an unmeasureable internal state.

For clarity and uniformity of presentation, let the constants f_C, f_v, and f_s be the Coulomb friction coefficient, the viscous coefficient and the maximum static friction constant (stiction) respectively. In the following, we shall give a list of commonly used friction models that are easy for controller design and computer simulation.

2.2.1. *Static friction* (*stiction*). At zero velocity, the static friction opposes all motion as long as the 'torque' is smaller in magnitude than the maximum stiction f_s, and is usually described by

$$f_m = \begin{cases} u, & |u| < f_s, \\ f_s \delta(\dot{x}) \operatorname{sgn}(u), & |u| \geqslant f_s, \end{cases} \tag{3}$$

where

$$\delta(\dot{x}) = \begin{cases} 1, & \dot{x} = 0, \\ 0, & \dot{x} \neq 0, \end{cases} \quad \operatorname{sgn}(u) = \begin{cases} +1, & u > 0, \\ 0, & u = 0, \\ -1, & u < 0. \end{cases} \tag{4}$$

In actual (numerical) implementation, the impulse function can be approximated differently such as triangular and rectangular as in the case of Karnopp's version of stiction.

In fact, stiction is not truly a force of friction, but a force of constraint in pre-sliding and behaves like a spring. For small motion, the elasticity of asperities suggests that the applied force is approximately proportional to the pre-sliding displacement

$$f_m = f_t x \delta(\dot{x}), \tag{5}$$

where f_t is the tangential stiffness of the contact, x is the displacement away from equilibrium position and $\delta(\dot{x})$ is used to describe the fact that stiction only occurs when it is at rest. Up to a critical force, breakaway occurs and true sliding begins. Breakaway has been observed to occur at the order of 2–5 μm in steel junctions and millimetre motion in robots for the arms act as levers to amplify the micron motion at the gear teeth. Pre-sliding displacement is of interest to the control community in extremely high-precision positioning. If sensors are not sensitive enough, we would only be able to observe the commonly believed stiction model (3).

2.2.2. *Coulomb friction* (*dry friction*). Independent of the area of contact, the Coulomb friction always opposes relative motion and is proportional to the normal force of contact. The Coulomb friction is described by

$$f_m = f_C \operatorname{sgn}(\dot{x}), \tag{6}$$

where $f_C = \mu |f_n|$ with μ being the coefficient of friction and f_n the normal force. The constant f_C is independent of the magnitude of the relative velocity.

2.2.3. *Viscous friction.* Viscous friction corresponds to the well lubricated situation, and is proportional to the velocity. It obeys the linear relationship

$$f_m = f_v \dot{x}. \tag{7}$$

2.2.4. *Drag friction.* Drag friction is caused by resistance to a body moving through a fluid (e.g. wind resistance). It is proportional to the square of velocity as described by

$$f_m = f_d |\dot{x}| \dot{x}. \tag{8}$$

When the speed of travel is small, this term is negligible. This term may not be neglected in the control of the hard disc drive because of the high-speed rotation of spindle motors.

Classical friction models are different combinations of static, Coulomb and viscous frictions as their basic building blocks.

2.2.5. *Exponential model.* In the paper by Bo and Pavelescu (1982), after reviewing several existing models, an exponential model incorporating Coulomb and viscous frictions was given as

$$f_m(\dot{x}) = f_C \operatorname{sgn}(\dot{x}) + (f_s - f_C) \exp\left[-\left(\frac{\dot{x}}{\dot{x}_s} \right)^{\delta} \right] + f_v \dot{x}, \tag{9}$$

where $\dot{x}_s$ and δ are empirical parameters. By choosing different parameters, different frictions can be realized (Armstrong *et al.* 1994). While the range of δ may be large, $\delta = 2$ gives the Gaussian exponential model (Armstrong 1990) which is nearly equivalent to the Lorentzian model (15). Gaussian models have the following different forms.

(*a*) The Gaussian exponential model with one break is given by

$$f_m(\dot{x}) = f_C \operatorname{sgn}(\dot{x}) + (f_s - f_C) \exp\left[-\left(\frac{\dot{x}}{\dot{x}_s} \right)^{2} \right] + f_v \dot{x}. \tag{10}$$

(*b*) The Gaussian exponential with two breaks is given by

$$f_m(\dot{x}) = f_C \operatorname{sgn}(\dot{x}) + f_v\dot{x} + f_{s_1} \exp\left[-\left(\frac{\dot{x}}{\dot{x}_{s_1}}\right)^2\right] + f_{s_2} \exp\left[-\left(\frac{\dot{x}}{\dot{x}_{s_2}}\right)^2\right]. \quad (11)$$

(*c*) The Gaussian exponential with two breaks and offsets is given by

$$f_m(\dot{x}) = f_C \operatorname{sgn}(\dot{x}) + f_v\dot{x} + f_{s_1} \exp\left(-\frac{(\dot{x}-\dot{x}_{10})^2}{\dot{x}_{s_1}^2}\right) + f_{s_2} \exp\left(-\frac{(\dot{x}-\dot{x}_{20})^2}{\dot{x}_{s_2}^2}\right), \quad (12)$$

where x_{s_1} and x_{s_2} are empirical parameters; f_{s_1} and f_{s_2} are static friction constants, and $\dot{x}_{10}$ and $\dot{x}_{20}$ are the offset points of breaks.

On the other hand, $\delta = 1$ gives the Tustin (1947) model as described by

$$f_m(\dot{x}) = f_C \operatorname{sgn}(\dot{x}) + (f_s - f_C) \exp\left[-\left(\frac{\dot{x}}{\dot{x}_s}\right)\right] + f_v\dot{x}. \quad (13)$$

The Tustin model is one of the best model describing the frictional force at velocities close to zero. It includes a decaying exponential term in the friction model. It explain the microscopic limit cycle behaviour, which, after a breakaway point at $\dot{x}$, has a negative exponential characterization. Experimental work has shown that this model can approximate the real frictional force with a precision of 90% (Armstrong 1988, Canudas de Wit and Carillo 1990).

Because of the nonlinearity in the unknown parameter $\dot{x}_s$ in the Tustin model and the difficulty in dealing with nonlinear parameters, the following simple LIP friction model was proposed (Canudas de Wit *et al.* 1991):

$$f_m(\dot{x}) = f_C \operatorname{sgn}(\dot{x}) + f_r(|\dot{x}|)^{1/2} \operatorname{sgn}(\dot{x}) + f_v\dot{x}, \quad (14)$$

where the constants f_i, $(i = C, r, v)$ are not unique and depends on the operating velocity. The simple LIP model has the following advantages.

(i) It captures the downward bends and possible asymmetrics.

(ii) The unknown parameters are linear and thus suitable for on-line identification.

(iii) These parameters can accommodate parametric changes due to environmental variations.

(iv) This type of model structure reduces the possibility of friction overcompensation resulting from estimation inaccuracies caused by simplified friction model structures such as the Coulomb friction and viscous friction model.

2.2.6. *Lorentzian model.* Hess and Soom (1990) employed a model of the form

$$f_m(\dot{x}) = f_C \operatorname{sgn}(\dot{x}) + (f_s - f_C)\frac{1}{1 + (\dot{x}/\dot{x}_s)^2} + f_v\dot{x}, \quad (15)$$

which shows a systematic dependence of $\dot{x}_s$ and f_v on the lubricant and loading parameters. In the same way as for the Gaussian model, the Lorentzian model also has the following forms with one break, with two breaks or with two breaks with offsets.

Remark 1: Based on the above discussion, a more complete model may consist of the following components: stiction, Coulomb, viscous, drag friction and square root friction, that is

$$f_m(x, \dot{x}) = f_t x\delta(\dot{x}) + f_C \operatorname{sgn}(\dot{x}) + f_v\dot{x} + f_d\dot{x}|\dot{x}| + f_r(|\dot{x}|)^{1/2} \operatorname{sgn}(\dot{x}), \quad (16)$$

which can be conveniently expressed in the LIP form as

$$f_m(x, \dot{x}) = S^T(x, \dot{x})P, \quad (17)$$

where

$$S(x, \dot{x}) = [x\delta(\dot{x}), \operatorname{sgn}(\dot{x}), \dot{x}, \dot{x}|\dot{x}|, (|\dot{x}|)^{1/2} \operatorname{sgn}(\dot{x})]^T \quad (18)$$

$$P = [f_t, f_C, f_v, f_d, f_r]^T, \quad (19)$$

where $S(x, \dot{x})$ is a vector of known basis functions, and P is the vector of unknown parameters. Although the LIP form is very desirable for model-based friction compensation as will be shown later, it is in no sense complete but a more complete representation. If other nonlinear components, such as the nonlinear exponential term $\exp[-(\dot{x}/\dot{x}_s)^\delta]$ and Lorentzian term $1/[1 + (\dot{x}/\dot{x}_s)^2]$ under the assumption of known $\dot{x}_s$ and δ, exist in the friction model, the space of the regressor function can be simply increased by including them in. If $\dot{x}_s$ and δ are not known, they can be approximated using the primitives explored by Canudas de Wit and Ge (1997).

Remark 2: It is generally considered to have two different manifestations, namely pre-sliding friction and sliding friction (Armstrong *et al.* 1994). In the pre-sliding stage, which is usually in the range of less than 10^{-5} m, friction is dominated by the elasticity of the contacting asperity of surfaces as described by (5). It not only depends on both the position and the velocity of motion but also exhibits nonlinear dynamic behaviour such as hysteresis characteristics with respect to the position and the velocity as observed by many researchers. In the sliding stage, friction is dominated by the lubrication of the contacting surfaces and introduces damping into the system. It is usually represented by various functions of the velocity. Thus, we can conclude that friction is continuous although it may be

extremely highly nonlinear and depends on both the position and the velocity. The discontinuities modelled by stiction (3) and Coulomb friction (6) are actually observation at the macroscopic level. Thus, friction can be approximated by neural networks as explained below.

2.2.7. *Neural network friction model.* Neural networks offer a possible tool for the nonlinear mapping approximation. A neural network can approximate any continuous function to arbitrarily any accuracy over a compact set if the size of the network is large enough (Lewis and Liu 1996).

Because of the complexity and difficulty in modelling friction, neural networks may be used to generate input–output maps using the property that a multi-layer neural network can approximate any function, under mild assumptions, with any desired accuracy. It has been proven that any continuous functions, not necessarily infinitely smooth, can be uniformly approximated by a linear combinations of Gaussian radial basis functions (RBF). The Gaussian RBF neural network is a particular network architecture which uses l Gaussian functions of the form

$$s_i(x,\dot{x}) = \exp\left(-\frac{(x-\mu_{1i})^2 + (\dot{x}-\mu_{2i})^2}{\sigma^2}\right), \qquad (20)$$

where x and $\dot{x}$ are the input variables, σ^2 is the variance, and μ_1 and μ_2 are the centres. A Gaussian RBF neural network can be mathematically expressed as

$$f_{\mathrm{m}}(x,\dot{x}) = S^{\mathrm{T}}(x,\dot{x})P, \qquad (21)$$

where $S(x,\dot{x}) = [s_1, s_2, \ldots, s_l]^{\mathrm{T}} \in R^l$ is the known basis function vector, and $P \in R^l$ is the corresponding weight vector. A general friction model $f(x,\dot{x})$ can then be written as

$$f(x,\dot{x}) = f_{\mathrm{m}}(x,\dot{x}) + \epsilon(x,\dot{x}), \qquad (22)$$

where $f_{\mathrm{m}}(x,\dot{x})$ is given in (21) and $\epsilon(x,\dot{x})$ is the neural network functional reconstruction error.

If there exist an integer l and a constant P such that $\epsilon = 0$, $f(x,\dot{x})$ is said to be in the functional range of the neural network. It is well known that any sufficiently smooth function can be approximated by a suitably large network using various activation functions, $\sigma(.)$, based on the Stone–Weierstrass theorem. Typical choices for $\sigma(.)$ include the sigmoid function, hyperbolic tangent function and RBFs. We only present LIP neural networks for ease of analysis and controller design later. Nonlinear multilayer neural networks can also be investigated following the work of Kim and Lewis (1998) and Ge *et al.* (1998 a).

It is clear that friction can be described by the general form $f(x,\dot{x}) = f_{\mathrm{m}}(x,\dot{x}) + \epsilon(x,\dot{x})$ where $f_{\mathrm{m}}(x,\dot{x}) = S^{\mathrm{T}}(x,\dot{x})P$ is the LIP model for friction and ϵ is the residue modelling error. If $S(x,\dot{x})$ consists of the classical model basis functions listed in (18), P is the corresponding coefficient vector. If S is the basis function vector of the neural network model (21), P is the neural network weight vector.

There are also other friction models in the literature although they cannot be conveniently or approximately expressed in the LIP form but may be able to describe the friction phenomenon more accurately such as the Z model (Canudas de Wit *et al.* 1995), the Karnopp (1985) model, the reset integrator model (Haessig and Friedland 1991) and the Dahl (1968) model. Because of limited space, the Z model is briefly discussed for completeness here.

2.2.8. *Z model.* There are several interesting properties observed in systems with friction that cannot be explained by classical models because the internal dynamics of friction are not considered. Examples of these dynamic properties are stick–slip motion, presliding displacement, the Dahl effect and frictional lag. All these static and dynamic characteristics of friction are captured by the Z model proposed by Canudas de Wit *et al.* (1995). The Z model considered the stiction behaviour. The model is based on the average of the bristle. The average deflection of the bristle is denoted by z and is modelled by

$$\frac{\mathrm{d}z}{\mathrm{d}t} = \dot{x} - \frac{|\dot{x}|}{g(\dot{x})}z. \qquad (23)$$

The frictional force accounts for Stribeck effect and viscous friction and is given by

$$f_{\mathrm{m}} = \sigma_0 z + \sigma_1 \frac{\mathrm{d}z}{\mathrm{d}t} + f_{\mathrm{v}}\dot{x}, \qquad (24)$$

where σ_0 and σ_1 are the stiffness and damping coefficient respectively. One parametrization of $g(\dot{x})$ to describe the Stribeck effect is

$$\sigma_0 g(\dot{x}) = f_{\mathrm{C}} + (f_{\mathrm{s}} - f_{\mathrm{C}})\exp\left[-\left(\frac{\dot{x}}{\dot{x}_{\mathrm{s}}}\right)^2\right]. \qquad (25)$$

Because of the difficulty in controller design using the Z model and the above nice properties in describing friction, it shall be used to describe the friction in the plant in our simulation studies. The internal dynamics are not compensated for explicitly in the controller.

3. Controller design

In the literature, many control techniques have been investigate for friction compensation, which include high-gain PID (Armstrong and Amin 1996), feedforward compensation (Cai and Song 1993), robust friction compensation (Ward *et al.* 1991, Cai and Song 1994),

adaptive friction compensation (Canudas de Wit *et al.* 1987, Canudas de Wit *et al.* 1991) and neural network control (Canudas de Wit and Ge 1997, Kim and Lewis 1998). In this work, we shall investigate a unified adaptive controller based on the parametrization techniques (model based and neural network based) presented previously which are LIP.

Let $x_d(t)$, $\dot{x}_d(t)$ and $\ddot{x}_d(t)$ be the position, velocity and acceleration respectively of the desired trajectory. Define the tracking errors as

$$e = x_d - x, \tag{26}$$

$$r = \dot{e} + \lambda e, \tag{27}$$

where $\lambda > 0$. Define the reference velocity and acceleration signals as

$$\dot{x}_r = \dot{x}_d + \lambda e, \tag{28}$$

$$\ddot{x}_r = \ddot{x}_d + \lambda \dot{e}. \tag{29}$$

Let $(\hat{*})$ be the estimate of $(*)$ and $(\tilde{*}) = (*) - (\hat{*})$. Then, we have $\hat{f}_m = S^T \hat{P}$, $\tilde{f}_m = S^T \tilde{P}$.

Consider the controller given by

$$u = \hat{m}\ddot{x}_r + \hat{f}_m + k_1 r + u_r + k_i \int_0^t r \, d\tau \tag{30}$$

where $k_1 > 0$ and u_r is a robust control term for suppressing any modelling uncertainty. First, let us consider the sliding mode control $u_r = k_2 \operatorname{sgn}(r)$.

The closed-loop system is then given by

$$m\dot{r} + k_1 r + u_r + k_i \int_0^t r \, d\tau = \tilde{m}\ddot{x}_r + \tilde{f}_m + d + \epsilon, \tag{31}$$

which can be further written as

$$m\dot{r} + k_1 r + u_r + k_i \int_0^t r \, d\tau = d + \epsilon + \ ^T\tilde{\theta}, \tag{32}$$

where $^T = [\ddot{x}_r, S^T]$ and $\tilde{\theta} = [\tilde{m}, \tilde{P}]^T$.

The closed-loop stability properties are then summarized in the following theorem.

Theorem 1: *The closed-loop system* (32) *is asymptotically stable if the parameters are updated according to*

$$\dot{\tilde{\theta}} = \Gamma \ r, \quad \Gamma^T = \Gamma > 0, \tag{33}$$

and the gain of the slide mode control $k_2 \geqslant |d + \epsilon|$.

Proof: Consider the positive definite Lyapunov function candidate

$$V = \tfrac{1}{2} m r^2 + \tfrac{1}{2} \tilde{\theta}^T \Gamma^{-1} \tilde{\theta} + \tfrac{1}{2} k_i \left(\int_0^t r \, d\tau \right)^2. \tag{34}$$

Its time derivative of V is given by

$$\dot{V} = mr\dot{r} + \tilde{\theta}^T \Gamma^{-1} \dot{\tilde{\theta}} + r k_i \int_0^t r \, d\tau. \tag{35}$$

Substituting (32) into (35) leads to

$$\begin{aligned} \dot{V} &= r(d + \epsilon + \ ^T\tilde{\theta} - k_1 r - u_r) + \tilde{\theta}^T \Gamma^{-1} \dot{\tilde{\theta}} \\ &= -k_1 r^2 + r(d + \epsilon - u_r) + r \ ^T\tilde{\theta} + \tilde{\theta}^T \Gamma^{-1} \dot{\tilde{\theta}}. \end{aligned}$$

Since θ is constant, and noting the adaptive law (33), we have

$$\dot{\tilde{\theta}} = -\Gamma \ r, \quad \Gamma^T = \Gamma > 0. \tag{36}$$

Combining the above two equations leads to

$$\dot{V} = -k_1 r^2 + r(d + \epsilon - u_r). \tag{37}$$

Since $u_r = k_2 \operatorname{sgn}(r)$ and $k_2 \geqslant |d + \epsilon|$, we have $\dot{V} = -k_1 r^2 \leqslant 0$.

It follows that $0 \leqslant V(t) \leqslant V(0)$, $\forall t \geqslant 0$. Hence $V(t) \in L_\infty$, which implies that $\tilde{\theta}$ is bounded. In other words, $\hat{\theta}$ is bounded for θ is a constant although unknown. Since $r \in L_2^n$, $e \in L_2^n \cap L_\infty^n$, e is continuous and $e \to 0$ as $t \to \infty$, and $\dot{e} \in L_2^n$. By noting that $r \in L_2^n$, x_d, $\dot{x}_d$, $\ddot{x}_d \in L_\infty^n$, and is of bounded functions, it is concluded that $\dot{r} \in L_\infty^n$ from (32). Using the fact that $r \in L_2^n$ and $\dot{r} \in L_\infty^n$, thus $r \to 0$ as $t \to \infty$. Hence $\dot{e} \to 0$ as $t \to \infty$. □

With regard to the implementation issues, we make the following remarks.

Remark 3: The presence of the sgn(.) function in the sliding mode control inevitably introduces chattering, which is undesirable as it may excite mechanical resonance and causes mechanical wear and tear. To alleviate this problem, many approximation mechanisms have been used, such as a boundary layer, saturation functions (Ge *et al.* 1998 b), and a hyperbolic tangent function $\tanh(\cdot)$, which has the following nice property (Polycarpou and Ioannou 1993):

$$0 \leqslant |\alpha| - \alpha \tanh\left(\frac{\alpha}{\varepsilon}\right) \leqslant 0.2785\varepsilon, \quad \forall \alpha \in R. \tag{38}$$

By smoothing the sgn(.) function, although asymptotic stability can no longer be guaranteed, the closed-loop system is still stable but with a small residue error. For example, if $u_r = k_2 \tanh(r/\epsilon_r)$, where $\epsilon_r > 0$ is a constant, and $k_2 \geqslant |d + \epsilon|$, then (37) becomes

$$\begin{aligned} \dot{V} &= -k_1 r^2 + r(d + \epsilon - u_r) \\ &\leqslant -k_1 r^2 + |r||d + \epsilon| - r k_2 \tanh\left(\frac{r}{\epsilon_r}\right) \\ &\leqslant -k_1 r^2 + |r| k_2 - r k_2 \tanh\left(\frac{r}{\epsilon_r}\right). \end{aligned} \tag{39}$$

Using (38), (39) can be further simplified as

$$\dot{V} \leqslant -k_1 r^2 + 0.2785 \epsilon_r k_2. \tag{40}$$

Obviously, $\dot{V} \leqslant 0$ whenever r is outside the compact set

$$D = \left\{ r | r^2 \leqslant \frac{0.2785\epsilon_r k_2}{k_1} \right\}. \tag{41}$$

Thus, we can conclude that the closed-loop system is stable and the tracking error will converge to a small neighbourhood of zero, whose size is adjustable by the design parameters k_1 and ϵ_r.

It should be mentioned that these modification may cause the estimated parameters grow unboundedly because asymptotic tracking cannot be guaranteed. To deal with this problem, the σ modification scheme or e modification among others (Ioannou and Sun 1996) can be used to modify the adaptive laws to guarantee the robustness of the closed-loop system in the presence of approximation errors. For example, $\hat{\theta}$ can be adaptively tuned by

$$\dot{\hat{\theta}} = \Gamma \ \ r - \sigma\hat{\theta}, \tag{42}$$

where $\sigma > 0$. The additional σ term in (42) ensures the boundedness of $\hat{\theta}$ when the system is subject to bounded disturbances without any additional prior information about the plant. The drawback of the smoothing method introduced here is that the tracking errors may only be made arbitrarily small rather than zero.

Remark 4: In this paper, only Gaussian RBF neural networks are discussed. In fact, other neural networks can also be used without any difficulty, which include other RBF neural networks, high-order neural networks (Ge *et al.* 1998 b), and multilayer neural networks (Lewis and Liu 1996, Zhang *et al.* 1999).

4. Simulation of friction compensation

In this section, simulation results are presented for illustrative purposes. The dynamics of the system are given by

$$m\ddot{x} + f = u, \tag{43}$$

$$f = \sigma_0 z + \sigma_1 \frac{\mathrm{d}z}{\mathrm{d}t} + f_v \dot{x}, \tag{44}$$

$$\frac{\mathrm{d}z}{\mathrm{d}t} = \dot{x} - \frac{|\dot{x}|}{g(\dot{x})} z. \tag{45}$$

The frictional force f considered here is represented by the Z model which captures most friction behaviours, and the factors in the model are chosen as $x_s = 0.001$, $\sigma_0 = 10^5$, $\sigma_1 = (10^5)^{1/2}$, $f_v = 0.4$. Although the system has internal dynamics, the controller does not explicitly compensate for it. The dynamic behaviour is approximately constructed using LIP models for ease of controller design. In this section, we shall show the effectiveness of the proposed approaches.

The desired trajectory is expressed as a sinusoidal function. The general expression for the desired position trajectory is

$$x_d(t) = 0.5 \sin(2\pi t). \tag{46}$$

The controller parameters are chosen as $\lambda = 50$, $k_i = 0$ and $\hat{\theta}(0) = 0$ under the assumption that no knowledge about the system is known. To show the robustness of the adaptive controller in the presence of approximation errors, we choose $k_2 = 0.0$.

4.1. *Conventional proportional–integral–derivative control*

For the purpose of comparison, consider first the control performance when the adaptation law is not activated by setting the adaptation gain $\Gamma = 0$. In this case, the resulting control action is effectively a conventional PID-type control.

$$u = k_1 r + k_i \int_0^t r \, \mathrm{d}\tau. \tag{47}$$

For comparison of low-gain and high gain feedback control, the following cases are selected: $k_1 = 10$, $k_1 = 30$, $k_1 = 50$, $k_1 = 100$, $k_1 = 200$ and $k_1 = 500$. The tracking performance for these cases are shown in figure 3, and the tracking errors are shown in figure 4, while the control signals are shown in figure 5.

It can be observed from these results that the low gain PID-type controller cannot control the system satisfactorily and large tracking errors exist. Although a high gain PID-type controller can reduce the tracking error as indicated, this is also not recommended in practice owing to the existence of measurement noise.

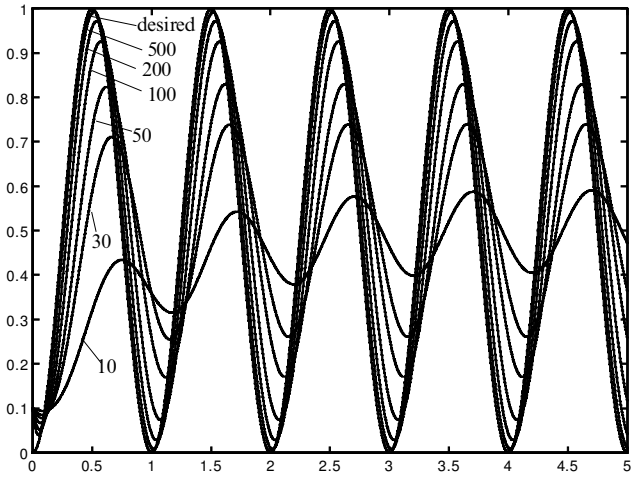

Figure 3. Tracking performance with different PD gains.

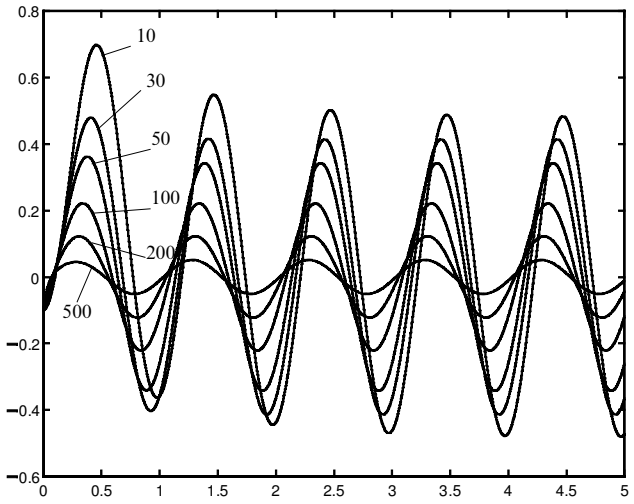

Figure 4. Tracking errors with different PD gains.

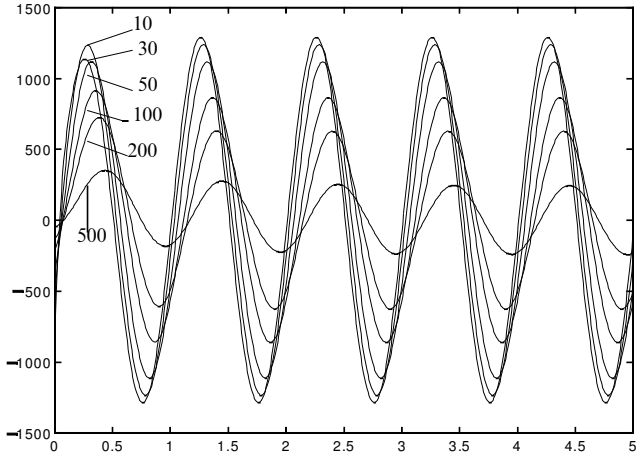

Figure 5. Control signals with different PD gains.

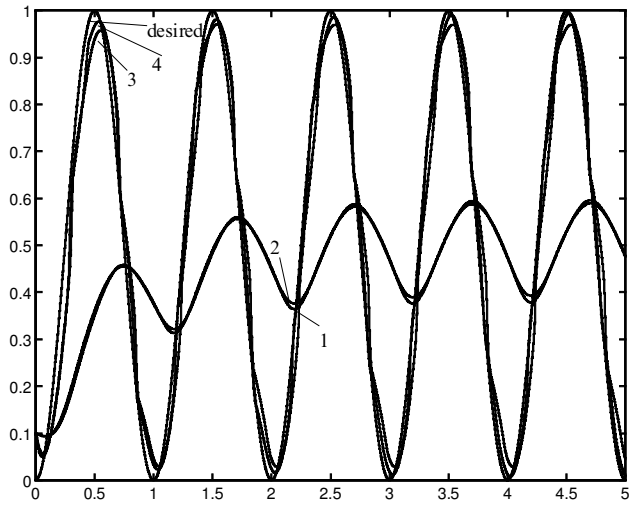

Figure 6. Tracking performance of model-based adaptive control.

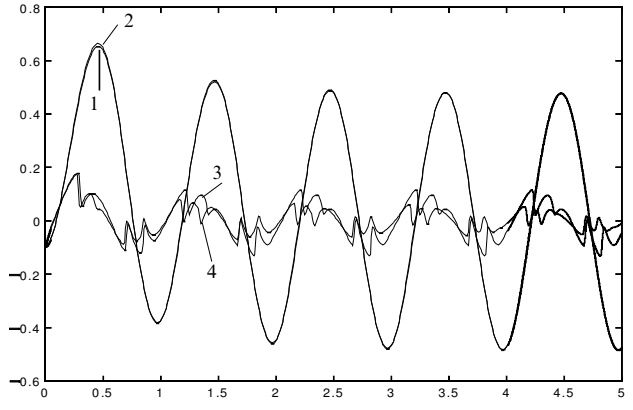

Figure 7. Tracking errors of model-based adaptive control.

4.2. *Model-based adaptive control*

For comparison, the complexity of the friction models also increases by augmenting the basis function space. The following different friction models have been chosen for analysis.

Case 1: $S = \mathrm{sgn}(\dot{x})$ and $P = f_C$.

Case 2: $S = [\mathrm{sgn}(\dot{x}),\ \dot{x}]^T$, and $P = [f_C, f_v]^T$.

Case 3: $S = [\mathrm{sgn}(\dot{x}),\ \dot{x},\ |\dot{x}|\dot{x}]^T$ and $P = [f_C, f_v, f_d]^T$.

Case 4: $S = [\mathrm{sgn}(\dot{x}),\quad \dot{x},\quad |\dot{x}|\dot{x},\quad |\dot{x}|^{1/2}\,\mathrm{sgn}(\dot{x})]^T$ and $P = [f_C, f_v, f_d, f_r]^T$.

For cases 1 and 2, the control feedback gain is chosen as $k_1 = 10$, and the adaptation mechanism is activated by choosing $\Gamma = \mathrm{diag}\,[0.1]$. The tracking performance and the tracking errors are shown in figures 6 and 7 respectively, while the corresponding control signals are shown in figure 8 by curves 1 and 2 respectively.

It was found that the system becomes unstable for high-gain feedback because the friction models are too simple to sufficiently approximate the Z model in the plant. The allowable feedback gain is $k_1 = 10$ for the two cases and a large tracking error exists. Because of the existence of a large tracking error, the gain of adaptation cannot be chosen too large either. If a high adaptive gain is chosen, the system may become unstable.

For cases 3 and 4, as the friction models become complex and capture the dominant dynamic behaviours, it was found that high feedback gains can be used and the speed of adaptation can be also be increased. For comparison studies, the tracking performance and the tracking errors are also shown in figures 6 and 7 respectively, while the corresponding control signals are shown

in figure 8, when $k_1 = 80$ and $\Gamma = \text{diag}\,[10]$, by curves 3 and 4 respectively. It can be seen that the tracking performance is much improved. The boundedness of the adaptive parameters are shown in figure 9.

4.3. *Neural-network-based adaptive control*

To show the effectiveness of neural-network-based adaptive control, the Gaussian RBF neural network of 100 nodes with $\sigma^2 = 10.0$ is chosen to approximate friction. For the controller, the following parameters are chosen: $k_1 = 10$ and $\Gamma = \text{diag}\,[100]$.

The tracking performance and the tracking error are shown in figures 10 and 11 respectively, while the control signals and neural network weights are shown in figures 12 and 13 respectively. It can be seen that the neural-network-based adaptive controller can produce good tracking performance and guarantees the boundedness of all the closed-loop signals because the neural network friction model can capture the dominate dynamic behaviour of the Z model in the plant.

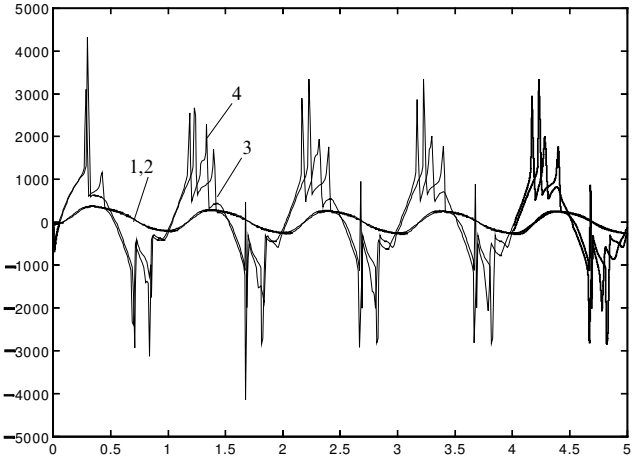

Figure 8. Control signals of model-based adaptive control.

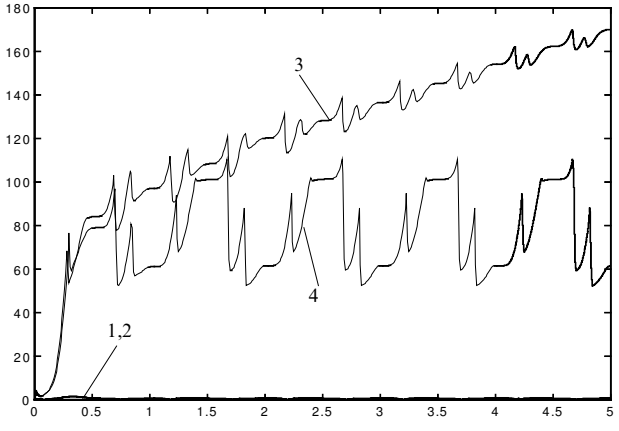

Figure 9. Variations in parameters.

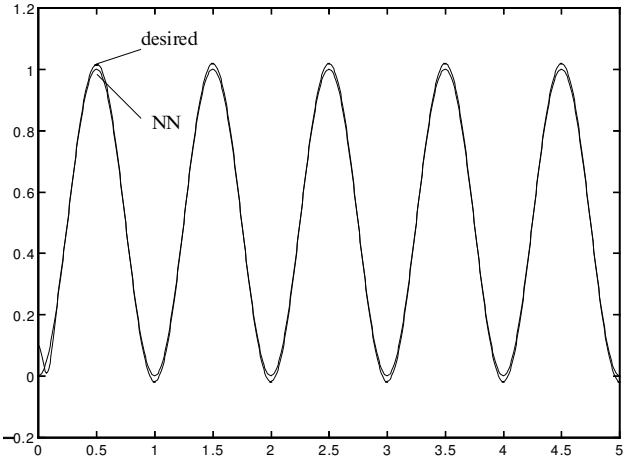

Figure 10. Tracking performance of adaptive neural network (NN) control.

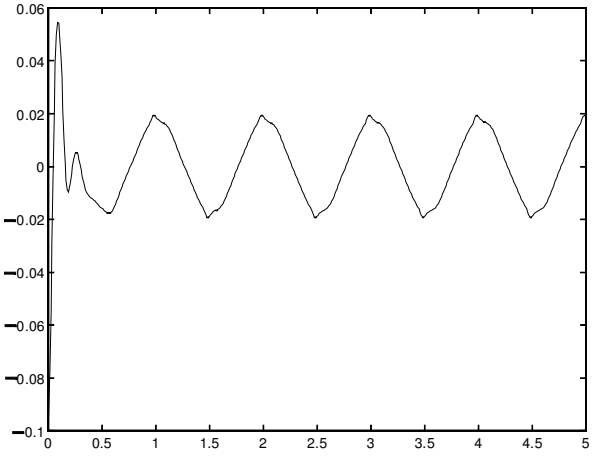

Figure 11. Tracking error of adaptive neural network control.

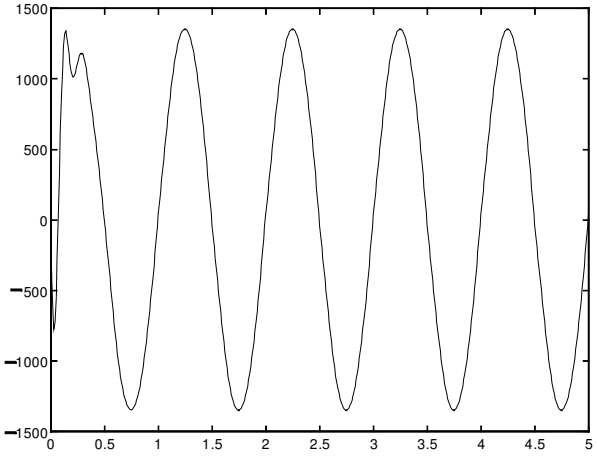

Figure 12. Control signals of adaptive neural network control.

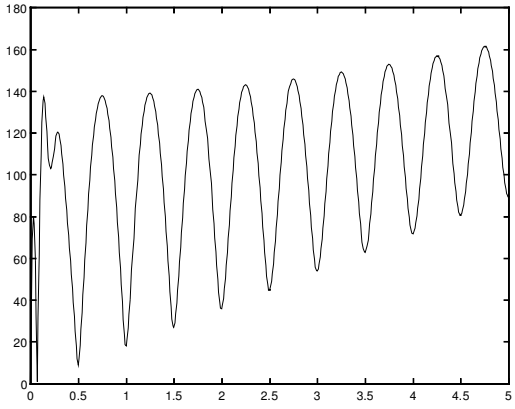

Figure 13. Variations in neural network weights.

5. Conclusions

In this paper, adaptive friction compensation has been investigated using both model-based and neural network (non-model-based) parametrization techniques. After a comprehensive list of commonly used models for friction has been presented, model-based and non-model-based adaptive friction controllers were developed with guaranteed closed-loop stability. Intensive computer simulations has been carried out to show the effectiveness of the proposed control techniques, and to illustrate the effects of certain system parameters on the performance of the closed-loop system. It has been observed that as the friction models become complex and capture the dominate dynamic behaviours, higher feedback gains for model based control can be used and the speed of adaptation can be also be increased for better control performance. It has also been found the neural networks are suitable candidate for friction modelling and adaptive controller design for friction compensation.

References

Annaswamy, A. M., Skantze, F. P., and Loh, A. P., 1998, Adaptive control of continuous time systems with convex/concave parameterization. *Automatica*, **34,** 33–49.

Armstrong, B., and Amin, B., 1996, PID control in the presence of static friction: a comparison of algebraic and describing function analysis. *Automatica*, **32,** 679–692.

Armstrong, B., Dupont, P. E., and Canudas, de Wit C., 1994, A survey of analysis tools and compensation methods for control of machines with friction. *Automatica*, **30,** 1083–1138.

Bo, L. C., and Pavelescu, D., 1982, The friction–speed relation and its influence on the critical velocity of the stick–slip motion. *Wear*, **3,** 277–289.

Cai, L., and Song, G., 1993, A smooth robust nonlinear controller for robot manipulators with joint job stick–slip friction. *Proceedings of the IEEE International Conference on Robotics and Automation* (New York: IEEE), pp. 449–454; 1994, Joint stick–slip friction compensation of robot manipulators by using smooth robust controller. *Journal of Robotic Systems*, **11,** 451–470.

Canudas de Wit, C., å ström, K. J., and Braun, K., 1987, Adaptive friction compensation in dc-motor drives. *IEEE Journal of Robotics and Automation*, **3,** 681–685.

Canudas de Wit, C., and Carillo, J., 1990, A modified EW–RLS algorithm for system with bounded disturbance. *Automatica*, **26,** 599–606.

Canudas de Wit, C., and Ge, S. S., 1997, Adaptive friction compensation for systems with generalized velocity/position friction dependency. *Proceedings of the 36th IEEE Conference on Decision and Control* (New York: IEEE), pp. 2465–2470.

Canudas de Wit, C., and Kelly, R., 1997, Passivity-based control design for robots with dynamic friction. *Proceedings of the Fifth IASTED International Conference Robotics and Manufacturing*, pp. 84–87.

Canudas de Wit, C., Noeöl, P., Auban, A., and Brogliato, B., 1991, Adaptive friction compensation in robot manipulators: low velocities. *International Journal of Robotics Research*, **10,** 189–199.

Canudas de Wit, C., Olsson, H., å ström, K. J., and Lischinsky, P., 1995, A new model for control of systems with friction. *IEEE Transactions on Automatic Control*, **40,** 419–425.

Dahl, P. R., 1968, A solid friction model. Report AFO 4695-67-C-0158, Aerospace Corporation, EI Segundo, California.

Dupont, P. E., 1994, Avoiding stick–slip through PD control. *IEEE Transaction on Automatic Control*, **39,** 1094–1097.

Ge, S. S., Hang, C. C., and Zhang, T., 1998 a, Nonlinear adaptive control using neural network and its application to CSTR systems. *Journal of Process Control*, **9,** 313–323.

Ge, S. S., Lee, T. H., and Harris, C. J., 1998 b, *Adaptive Neural Network Control of Robotic Manipulators* (World Scientific, London).

Haessig, D. A., and Friedland, B., 1991, On the modeling and simulation of friction. *Journal of Dynamic Systems, Measurement and Control*, **113,** 345–362.

Hess, D. P., and Soom, A., 1990, Friction at a lubricated line contact operating at oscillating sliding velocity. *Journal of Tribology*, **112,** 147–152.

Ioannou, P. A., and Sun, J., 1996, *Robust Adaptive Control* (Englewood Cliffs, New Jersey: Prentice-Hall).

Karnopp, D., 1985, Computer simulation of stick–slip friction in mechanical dynamic system. *Journal of Dynamic Systems, Measurement and Control1,* **107,** 100–103.

Kim, Y. H., and Lewis, F. L., 1998, Reinforced adaptive learning neural network based friction compensation for high speed and precision. *Proceedings of the 37th IEEE Conference on Decision and Control* (New York: IEEE), pp. 16–18.

Lewis, F. L., and Liu, K., 1996, Multilayer neural-net robot controller with guaranteed tracking performance. *IEEE Transaction on Neural Network*, **2,** 188–198.

Polycarpou, M. M., and Ioannou, P. A., 1993, A robust adaptive nonlinear control design. *Proceedings of the American Control Conference*, pp. 1365–1369.

Tustin, A., 1947, The effects of backlash and of speed-dependent friction on the stability of closed-cycle control systems. *Journal of the Institution of Electrical Engineers*, **94,** 143–151.

Ward, S., Radcliff, S. C., and MacCluer, C. J., 1991, Robust nonlinear stick–slip friction compensation. *Journal of Dynamic Systems, Measurement, and Control*, **113,** 639–645.

Zhang, T., Ge, S. S., and Hang, C. C., 1999, Design and performance analysis of a direct adaptive controller for nonlinear systems. *Automatica*, **35,** 1809–1817.